



Surface properties of copper based cermet materials

M. Voinea*, C. Vladuta, C. Bogatu, A. Duta

The Centre: Product Design for Sustainable Development, Transilvania University of Brasov, Eroilor 29, 500036, Romania

ARTICLE INFO

Keywords:

Selective coatings
Copper based cermets
Spray pyrolysis deposition
Electrodeposition
Contact angle

ABSTRACT

The paper presents the characterization of the surface properties of copper based cermets obtained by two different techniques: spray pyrolysis deposition (SPD) and electrodeposition. Copper acetate was used as precursor of Cu/CuO_x cermet. The surface morphology was tailored by adding copolymers of maleic anhydride with controlled hydrophobia. The films morphology of Cu/CuO_x was assessed using contact angle measurements and AFM analysis. The porous structures obtained via SPD lead to higher liquid adsorption rate than the electrodeposited films. A highly polar liquid – water is recommended as testing liquid in contact angle measurements, for estimating the porosity of copper based cermets, while glycerol can be used to distinguish among ionic and metal predominant structures. Thus, contact angle measurements can be used for a primary evaluation of the films morphology and, on the other hand, of the ratio between the cermet components.

© 2008 Elsevier B.V. All rights reserved.

1. Introduction

To be efficient, solar thermal collectors use a spectrally selective surface that absorbs and converts the solar radiation into heat. Cermet materials are one of the high performing selective surfaces due to their optical properties: maximum absorption coefficient ($\alpha > 0.9$) in the wavelength (λ) range of 0.3–2.5 μm and minimum emissivity ($\varepsilon > 0.1$) in the infrared region ($\lambda > 2.5 \mu\text{m}$). They consist of metal particles embedded in a ceramic matrix, deposited on a metal substrate. Optimum cermet design requires a porous matrix for the metal infiltration.

Copper based cermets Cu/CuO_x can be used as selective coatings due to its good optical properties, good adhesion to metal surfaces, thermal and chemical stability. Different deposition techniques have been reported for copper oxide thin films (e.g. electrodeposition [1], sol–gel [2,3], cathodic arc deposition [4], pulsed magnetron sputtering [5], spray pyrolysis deposition (SPD) [6,7]. The SPD technique is a promising method due to its low cost and the possibility of depositing large area of thin films.

Contact angle measurements can be used to analyse the wetting behaviour and surface morphology. A wetting liquid is considered to be the one that produces a contact angle of 30° or less on a solid (Fig. 1a). Between 30° and 89° the liquid is partially wetting the solid (Fig. 1b) and above 90° the liquid presents non-wetting behaviour (Fig. 1c) [8]. By studying the contact angle time dependence

assumptions regarding the solid–liquid interactions and the solid morphology can be done. The contact angle is strongly decreasing for porous materials due to the liquid absorption/adsorption into the pores, while for dense films a slow variation of the contact angle in time is expected [9]. The surface charge of the solid also plays an important role and depends on the chemical bonds and, in some degree, on the morphology (smooth, fractured, etc.).

The aim of the experiments was to develop Cu/CuO_x cermet with controlled morphology, using SPD and electrodeposition, the latest considered as reference technique [10]. The cermet can be obtained on metallic substrate with the both techniques [11], but in this paper only the ceramic part deposited by SPD was studied, and the cermet obtained by electrodeposition. For this purpose, the copper oxides were deposited on glass substrate in order to avoid the interfering from the oxides formed by thermal oxidation of the metallic (copper) substrate. Correlations between the film morphology and the contact angle values are developed; parallel analyses on the surface morphology were performed using atomic force microscopy (AFM). The influence of copper based cermet components (copper, copper oxides) on the surface energy is investigated.

2. Experimental

2.1. Samples preparation

Thin films of copper oxide were deposited by SPD onto microscopic glass from precursor solutions of (CH₃COO)₂Cu 0.1 M (Merck) in aqueous–ethanolic = 1:1 solvent (ethanol absolute,

* Corresponding author. Tel.: +40 268 475597; fax: +40 268 475597.
E-mail address: m.voinea@unitbv.ro (M. Voinea).

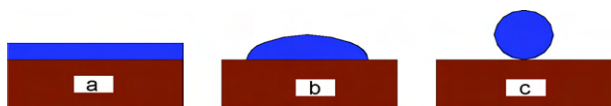


Fig. 1. The wetting behaviour.

Table 1

Deposition conditions for SPD and electrodeposition

Spray pyrolysis deposition			Electrodeposition		
Sample	T ($^{\circ}\text{C}$)	Complexing agent ^a	Sample	$E_{\text{deposition}}$ (V)	$t_{\text{deposition}}$ (min)
1	150	–	7	–0.16	20
2	150	Hfb	8	–0.65	10
3	200	–	9	–0.3	20
4	200	Hfb			
5	250	–			
6	250	Hfb			

^a Complexing agent: copolymers of maleic anhydride, the hydrophobic form.

Sharlau Chemie, S.A.). Copolymers of maleic anhydride with controlled hydrophobia, 50 ppm (synthesized at Petru Poni Institute, Romania) were added in the spraying solutions. The glass substrates ($1.5\text{ cm} \times 3\text{ cm}$, Heinz Herenz) were cleaned with ethanol before each deposition, in an ultrasonic bath. The substrate temperature (T) was varied during deposition from 150 to 250°C . Air was used as carrier gas ($p = 1.4\text{ bar}$). The deposition was done in open atmosphere, at a spraying angle of 45° . The distance from nozzle to the heated substrate was 20 cm and the spraying sequences number was 60.

For the electrodeposited films, the substrate – $1.5\text{ cm} \times 3\text{ cm}$ flat pieces of copper (99.9%) – was chemically cleaned with concentrated HNO_3 . A multichannel potentiostat galvanostat, PAR BioLogic VSP with a three-electrode system (working electrode: sample, counter electrode: platinum plate, reference electrode: $\text{Ag}/\text{AgCl}/\text{KCl}$ sat (SAE), $E_{\text{SAE}} = 0.197\text{ V}$) was used. All the potential were recorded versus SAE. The samples were obtained at room temperature, at different deposition potentials and durations, from precursor solutions based on mixtures of $(\text{CH}_3\text{COO})_2\text{Cu}$ 0.05 M with CH_3COONa 0.1 M. Table 1 presents the deposition parameters for both deposition techniques.

2.2. Characterization techniques

Contact angle measurements were performed at room temperature with the OCA-20 System (DataPhysics Instruments). The test liquids were: glycerol (Reactivul București) and ultra pure water (Direct-Q 3 Water Purification System). The surface tension, density and viscosity of these liquids are presented in Table 2. A $5\text{ }\mu\text{L}$ drop of liquid was placed on the sample with $1\text{ }\mu\text{L}/\text{s}$ velocity and the contact angles were measured by analyzing the droplet image, each second. The interaction energy was evaluated from the linear fit of the contact angle time dependence.

Infrared spectroscopy was used to determine the modifications in the precursor composition and the additives form depending on temperature. FT-IR measurements (Spectrum BX PerkinElmer) were done in reflectance mode, in the range of $500\text{--}4500\text{ cm}^{-1}$, after four scans, with 4 cm^{-1} resolution.

Table 2

The properties of the liquids used for contact angle determination

Liquid properties	Distilled water [18]	Glycerol [19]
Surface tension, γ (mN/m)	72.10	63.40
Density, ρ (g/cm^3)	0.9982	1.2613
Viscosity, η (mPa s)	1.002	1412.0

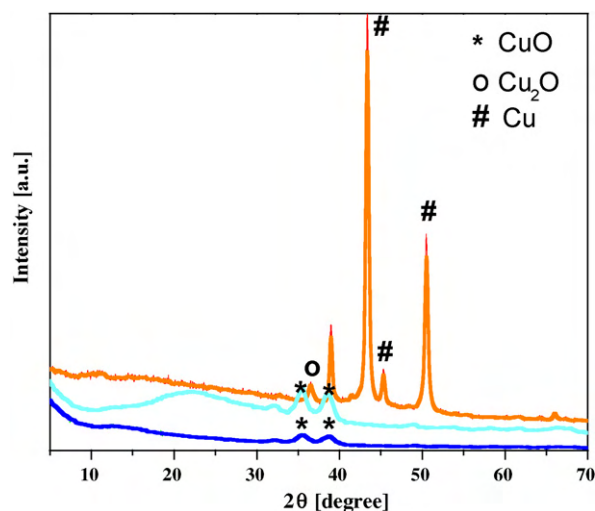


Fig. 2. XRD patterns for SPD (1, 2) and electrodeposited (7) samples.

Surface morphology and thin films roughness were examined using atomic force microscopy (NT-MDT model NTEGRA PRIMA EC). The images were taken in semi-contact mode with “GOLDEN” silicon cantilever (NCSG10, force constant 0.15 N/m , tip radius 10 nm).

X-ray diffraction (XRD, Bruker-AXS D8 Advance) was used to evaluate the films' crystalline structure and composition.

3. Results and discussion

3.1. Structural analyses

The XRD patterns recorded for Cu/CuO_x films deposited via SPD on microglass (Fig. 2) show crystalline CuO . All the diffraction peaks matched with the peaks from the monoclinic cuprite standard (PDF 48–1548). The crystalline structure is not influenced by the complexing agents, as confirmed by the XRD patterns. The electrochemically deposited films contain mainly Cu and Cu_2O . All the diffraction peaks can be indexed to the cubic structure Cu_2O (PDF 71–3645) and face-centered cubic Cu . The strong and sharp peaks suggested that more crystalline compounds are formed by electrodeposition.

3.2. Atomic force microscopy

Depending on the deposition parameters (substrate temperature, precursor composition – additives), different surface morphology were obtained (Figs. 3–6). The film, mainly consisting of CuO deposited from precursors without additives, Fig. 3, shows a uniform structure with columnar crystallites of $150\text{--}200\text{ nm}$

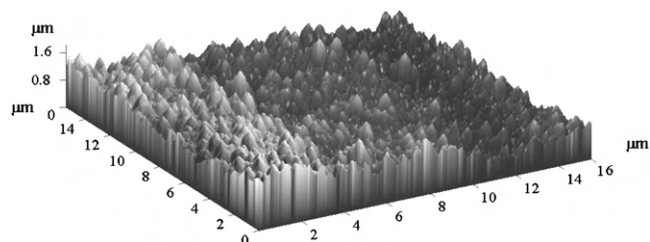


Fig. 3. AFM 3D surface morphology of SPD sample grown at $T = 150^{\circ}\text{C}$, without the addition of the complexing agents in the precursor solution, average roughness 204.7 nm .

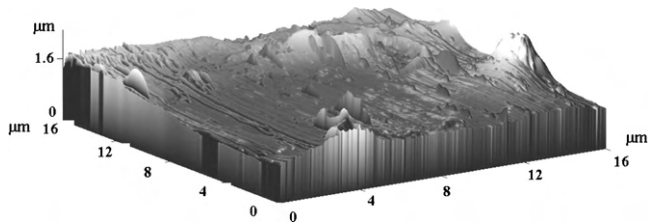


Fig. 4. AFM 3D surface morphology of SPD sample grown at $T=200^{\circ}\text{C}$, without the addition of the complexing agents in the precursor solution, average roughness 160.1 nm.

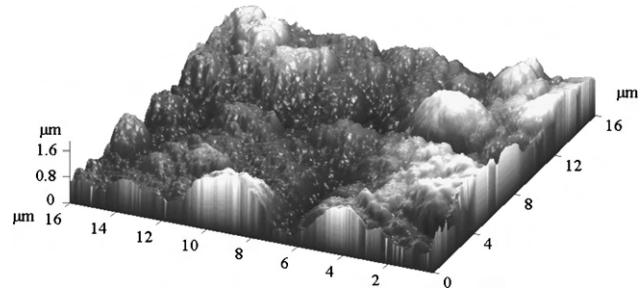


Fig. 5. AFM 3D surface morphology of SPD sample grown at $T=150^{\circ}\text{C}$, with complexing agents addition in the precursor solution; average roughness 198.2 nm.

diameter and average roughness of 204.7 nm. Higher deposition temperatures (Fig. 4), result in completely different, compact, smoother structures (average roughness: 160.1 nm). Increasing the growth temperature increases the effective diffusion length of depositing species resulting to smoother films. The surface morphology is also controlled by adding copolymers of maleic anhydride as complexing agents into the spraying solution. The polar CO groups in the copolymer can interact with the copper ions in the precursor's phase leading to intermediate components [12,13] that react slower in the nucleation step, thus forming an open porous matrix of meso- and micro-structured associated crystallites (Fig. 5) with lower roughness values: 198.2 nm. Films with uniform morphologies, but with higher roughness (289.8 nm) are obtained via electrodeposition (Fig. 6). The film roughness was evaluated based on the AFM analysis. Experiments show that electrodeposited Cu/CuO_x is preferential depositing on the high-energy sites (edges and corners) of the substrate; therefore, the substrate morphology and the deposition time have a strong influence on the film growth. Longer deposition times are required for uniform coverage of the metallic substrate.

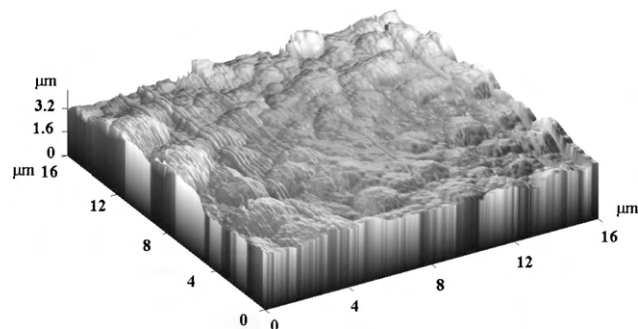


Fig. 6. AFM 3D surface morphology for the electrodeposited sample (at -0.3 V , for 20 min); average roughness 289.8 nm.

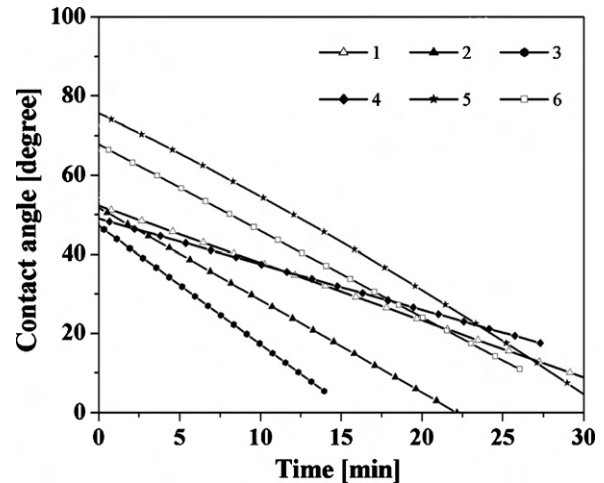


Fig. 7. Time dependence of contact angle measured with water for the SPD samples.

3.3. Fourier transform infra-red (FT-IR) analysis

Possible interaction mechanism between the metal precursor and the maleic anhydride copolymers with controlled water solubility were studied based on FT-IR analysis. The IR studies were performed for aqueous solutions of the polymers and Cu^{2+} precursor, at room temperature and at 50°C . Interactions between the copper ions with the $\text{C}=\text{O}$ anhydride groups were identified in solution; the characteristic bands are located in a wide spectral interval, from 2236 to 2150 cm^{-1} [14]. At higher temperatures (50°C), the presence of the COO^- groups resulted from the hydrolysis of the ester groups was registered (1730 and 1244 cm^{-1}) [15].

3.4. Contact angle analysis

The interaction between the different liquids and the film surface was evaluated based on contact angle measurements. The contact angle values vary with the film surface charge and porosity, and with the liquid polarity. The slopes of the contact angle vs. time function may be correlated with the absorption (characteristic to large pores morphology – when a high decrease in time of the contact angle is expected) and/or adsorption rate of the liquid on/in the film (in the case of nano- or meso-pores).

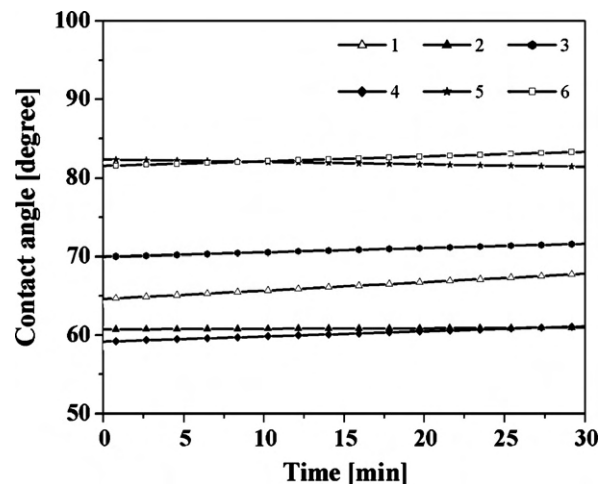


Fig. 8. Time dependence of contact angle measured with glycerol for the SPD samples.

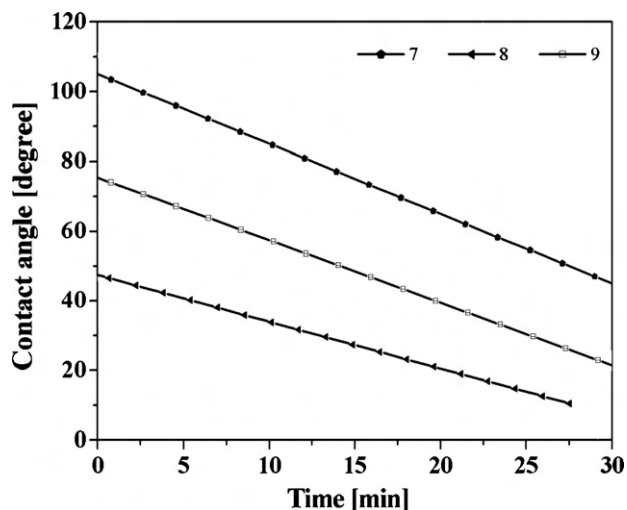


Fig. 9. Time dependence of contact angle measured with water for the electrodeposited samples.

The oxides containing metal particles with inferior oxidation state (Cu_2O) present a higher ionic character than oxides containing metal ions in higher oxidation states (CuO) [16,17]. Thus, stronger interactions between Cu_2O –water are expected.

The contact angle measurements at initial moment ($t=0$ s) show large variation for the SPD deposited samples, as result of the different morphologies. Dense morphologies, obtained at the highest deposition temperature (sample 5 and sample 6) have the contact angle value with about 30% higher than the other samples, confirming the dense structures obtained. The porous structures tailored using the polymer additives, present lower contact angle (θ) values (for all the analysed samples). The slope of the θ vs. time variation must be correlated with the film morphology and with the chemical composition. Samples obtained at the same temperature with and without additives show, at lower deposition temperatures, different slopes that could be attributed to the by-products resulted, in different quantities, from the precursor's thermal degradation. These products, embedded in the film, have different polarity, caused by the different reaction temperatures; lower deposition temperatures favour the formation of low polarity substances while increasing the temperature, carboxilates can be formed, as confirmed by the FT-IR analysis.

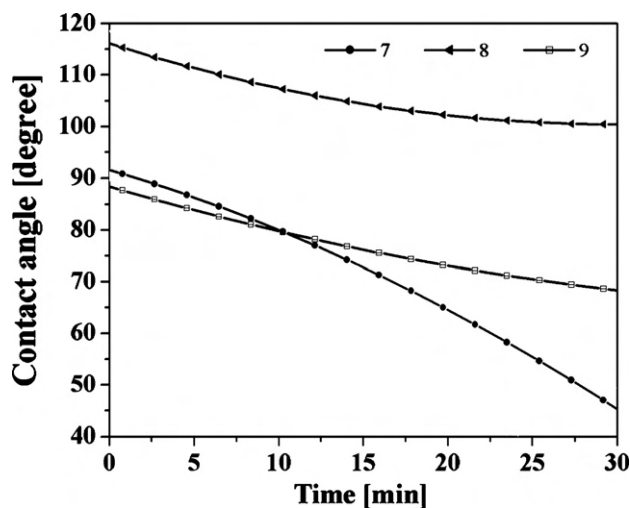


Fig. 10. Time dependence of contact angle measured with glycerol for the electrodeposited samples.

Table 3

The correlations between contact angle interparticle bonds for the electrodeposited samples

Sample	7	8	9
Composition	Cu_2O	Cu	$\text{Cu}_2\text{O}/\text{Cu}$
Interparticle bonds	Predominant ionic	Metallic	Ion-metal
θ (degree)	104.71	75.26	47.43

Glycerol, with lower polarity, is expected to have weaker interaction with the predominant ionic structures, comparing with water, thus higher contact angles. The results presented in Figs. 7–10 confirm this assumption. For the samples with predominant Cu_2O content, there is practically no variation of the contact angle in time, showing that glycerol is not suited for estimating the morphology variations of these thin layers.

For the electrodeposited samples, the contact angle depends on the copper/copper oxide ratio. Previous studies showed that at $E = -0.16$ V, Cu_2O is mainly deposited, at $E = -0.65$ V, copper is obtained, while at $E = -0.3$ V a mixture of copper and Cu_2O with different ratios is formed [11]. These compositions are confirmed by the contact angle values, at $t=0$ s, in the water-film systems, Table 3 and Fig. 9.

Glycerol contact angle non-linear behaviour, Fig. 10, indicates a complex of processes occurring in time; the similar behaviour of sample 8 and 9 can indicate a predominant metal content in the cermet, but further investigations are required.

4. Conclusions

The films morphology of Cu/CuO_x was assessed using two different techniques: contact angle measurements and AFM analysis.

Open, large pore structures can be correlated with the initial value of the contact angle and with the adsorption rate of a liquid in the pores that can be visualized by the decrease in time of a drop on the substrate, i.e. with the modification (decrease) of the contact angle.

The liquid suited for indirect morphology characterisation must exhibit a sharp slope of the $\theta = f(\text{time})$ function. Experiments testing water (highly polar) and glycerol (low polar liquid) recommend water as a testing liquid for estimating the porosity of different, predominant ionic films with similar compositions. The contact angle can also be an interesting tool in investigating the film composition; tests done on $\text{Cu}/\text{Cu}_2\text{O}$ cermets with different metal content proved that glycerol can sense differences among ionic and metal predominant structures.

Acknowledgments

The research work was supported by the CNCSIS Td 312/2007 programme. The authors are grateful to Petru Poni Institute of Macromolecular Chemistry for providing the complexing agent and to ICPE-CA for the support in XRD characterization.

References

- [1] R.P. Wijesundara, L.D.R.D. Perera, K.D. Jayasuriya, W. Siripala, K.T.L. De Silva, A.P. Samantilleke, I.M. Dharmadasa, Solar Energy Materials & Solar Cells 61 (2000) 277.
- [2] S.C. Ray, Solar Energy Materials & Solar Cells 68 (2001) 307.
- [3] L. Armelao, D. Barreca, M. Bertapelle, G. Bottaro, C. Sada, E. Tondello, Thin Solid Films 442 (2003) 48.
- [4] A. Márquez, G. Blanco, M.E. Fernandez de Rapp, D.G. Lamas, R. Tarulla, Surface and Coatings Technology 187 (2004) 154.
- [5] E.M. Alkoya, P.J. Kelly, Vacuum 79 (2005) 221.
- [6] Y.S. Chaudhary, A. Agrawal, R. Shrivastav, V.R. Satsangi, S. Dass, International Journal of Hydrogen Energy 29 (2004) 131.

- [7] S.A. Nasser, H.H. Afify, S.A. El-Hakim, M.K. Zayed, *Thin Solid Films* 315 (1998) 327.
- [8] D. Mayer, *Surfaces, Interfaces, and Colloids: Principles and Applications*, 2nd ed., Wiley, New York, 1999, p. 415.
- [9] C. Vladuta, L. Andronic, M. Visa, A. Duta, *Surface and Coatings Technology* 202 (2007) 2448.
- [10] R.P. Wijesundera, M. Hidaka, K. Koga, M. Sakai, W. Siripala, *Thin Solid Films* 500 (2006) 241.
- [11] M. Voinea, C. Bogatu, G.C. Chitanu, A. Duta, *Rev. Chim. (Bucuresti)* 59 (2008) 659.
- [12] B.L. Rivas, L.N. Schiappacasse, U.E. Pereira, I. Moreno-Villoslada, *Polymer* 45 (2004) 1771.
- [13] S.K. Chatterjee, S. Gupta, K.R. Sethi, *Angewandte Makromolekulare Chemie* 147 (2003) 133.
- [14] A. Jagminas, G. Niaura, J. Kuzmarskytė, R. Butkienė, *Applied Surface Science* 225 (2004) 302.
- [15] A.T. Balaban, M. Banciu, I. Pogany, *Applications of the Physical Methods for Organic Chemistry*, Editura Stiintifica si Enciclopedica, Bucuresti, 1983, p. 31.
- [16] J.-K. Kim, R.S.C. Woo, P.Y.P. Hung, M. Lebbai, *Surface and Coatings Technology* 201 (2006) 320.
- [17] A. Klonkowski, *Journal of Non-Crystalline Solids* 57 (1983) 339.
- [18] H.J. Busscher, et al., *Colloids and Surfaces* 9 (1984) 319.
- [19] F.M. Fowkes, *Industrial and Engineering Chemistry* 56 (1964) 40.